ACOUSTICS 2012

Identification of the acoustic component in the turbulent boundary layer excitation by the Force Analysis Technique

D. Lecoq, C. Pezerat, J.-H. Thomas and W. Bi

Laboratoire d'acoustique de l'université du Maine, Bât. IAM - UFR Sciences Avenue Olivier Messiaen 72085 Le Mans Cedex 9
damien.lecoq@univ-lemans.fr

Turbulent flows, due to the presence of obstacles or turbulent boundary layers near the structure, generate vibrations and can be a major source of noise. This kind of excitation has two components: the aerodynamic and the acoustic parts respectively in the high and low wavenumbers. The vibrations and acoustic radiations of the wall are more sensitive to the acoustic component. Indeed, the wavelengths of the aerodynamic part are very small and they excite modes with low radiation. However, the aerodynamic part has a very high amplitude, so that the acoustic component becomes very difficult to assess by measurement.
The study aims at using the Force Analysis Technique (FAT), also known by its french acronym RIFF (Résolution Inverse Filtrée Fenêtrée), to measure these excitations. In this work, the acoustic pressure identification is tested by performing a numerical experiment where the excitation is obtained by a synthesis method of time signals using the Cholesky decomposition of the cross-spectra matrices.
The results obtained from the filtering done in the wavenumber domain by the Force Analysis Technique, show that the acoustic component can be extracted even if its energy level is very small with respect to that of the aerodynamic component.

1 Introduction

Turbulent Boundary Layers (TBL) are vibration sources composed of two components (Figure 1): the aerodynamic part due to the pressure fluctuations of the turbulences and the acoustic part corresponding to the radiation of the turbulences [1]. The first, represented by an ellipse in the wavenumber domain (Figure 2), is characterized by

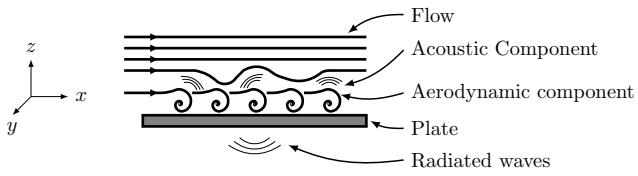

Figure 1: Plate excited by a Turbulent Boundary Layer.

$$k_{conv} = \frac{\omega}{U_c}, \tag{1}$$

the convection wavenumber where U_c is the convection velocity. The second component excites wavenumbers within the circle of radius k_{ac}, the acoustic wavenumber (Figure 2):

$$k_{ac} = \frac{\omega}{c_0}, \tag{2}$$

where c_0 is the sound speed. Although it depends on the studied cases, the acoustic component is always much smaller than the aerodynamic part [2, 3]. However, vibration and acoustic radiation of the plate are more sensitive to the acoustic component because the acoustic wavenumber k_{ac} is closer to the flexural wavenumber k_f (Figure 2):

$$k_f = \sqrt[4]{\frac{12\rho(1-\nu^2)}{Eh^2}}\,\sqrt{\omega}, \tag{3}$$

where ρ, E, ν are respectively the mass density, the Young's modulus, the Poisson's ratio of the material and h is the thickness of the plate.

The Force Analysis Technique (FAT) [4] is an inverse problem of vibration, based on the motion equation of a plate

$$\rho h \frac{\partial^2 w}{\partial t^2} + D\left(\frac{\partial^4 w}{\partial x^4} + \frac{\partial^4 w}{\partial y^4} + 2\frac{\partial^4 w}{\partial x^2 \partial y^2}\right) = F(x,y,t), \tag{4}$$

with $w(x,y,t)$ the displacement field, $F(x,y,t)$ the force distribution and $D = \frac{Eh^3}{12(1-\nu^2)}$. In the FAT, the spatial derivatives are estimated by the finite difference method. FAT is proposed to be used to measure this excitation. The goal is to identify the acoustic component wich is very difficult to assess by measurement because of its low level.

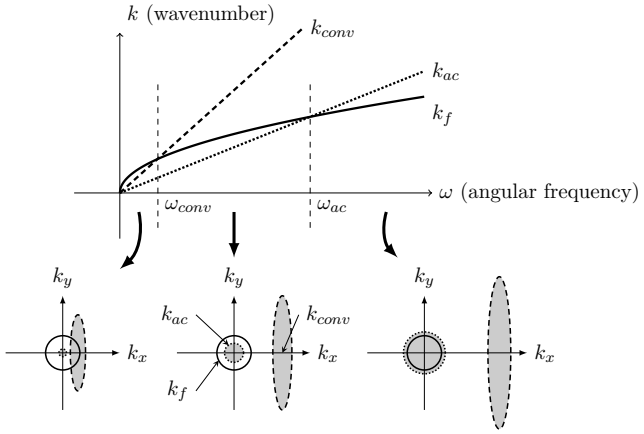

Figure 2: Flexural, convection and acoustic wavenumbers with respect to the angular frequency ω and for low Mach numbers. Energy distribution of the excitation in the wavenumber domain [1, 2].

A numerical experiment is performed to test the identification of TBL by this method. Section 2 describes the TBL model and the associated method of synthesis which leads to the excitation signals used for the direct problem of vibration. Section 3 presents the turbulent wall pressures identified by FAT in the inverse problem.

2 Turbulent Boundary Layer excitation: model and synthesis

TBL are generally characterized by their frequency and wavenumber-frequency spectra. The first, denoted by $S_{pp}(\omega)$, represents the energy distribution of the excitation in the frequency domain [5]. The second is the spatial Fourier transform of the cross-spectrum $S_{pp'}(r_x, r_y, \omega)$ between two points p and p', and reflects the spatial correlations [6]. It is denoted $S_{pp'}(k_x, k_y, \omega)$.

In this study, the chosen frequency spectrum is the semi-empirical model of Goody. Indeed, it seems to fit the experimental results in the best way (the most accurately) [5]:

$$S_{pp}(\omega) = \frac{3\tau_w^2 \delta \left(\frac{\omega\delta}{U_\infty}\right)^2}{U_\infty\left(\left[0.5 + \left(\frac{\omega\delta}{U_\infty}\right)^{0.75}\right]^{3.7} + \left[1.1\, R_T^{-0.57}\left(\frac{\omega\delta}{U_\infty}\right)\right]^7\right)}, \tag{5}$$

where u_*, δ, ν', τ_w are respectively the friction velocity, the boundary layer thickness, the kinematic coefficient of viscosity and the wall shear stress. The parameter $R_T = \frac{u_*^2 \delta}{\nu' U_\infty}$ is defined in order to take into account the Reynolds number. Some values of these coefficients are given by Hwang *et al.* [5].

For the cross-spectrum, there are several types of models that can take into account the compressibility of the fluid and therefore the acoustic component:

- Theoretical models based on the Navier-Stokes equations such as the Direct Numerical Simulation (DNS). But these methods are very restrictive in terms of computational cost [7] ;
- Semi-empirical models, like Chase (1987) [8] based on the Poisson's equation. However, these models must be adjusted by coefficients to be estimated experimentally, which is complicated in the low wavenumbers because the measurement of the acoustic component is too difficult.

The aim of this work is not to model precisely the excitation but see how FAT identifies the pressure whose cross-spectrum is similar to that of the TBL. Thus a simplified model [3] is used. It combines a Corcos field [9]

$$S_{pp'}^{aero}(r_x, r_y, \omega) = S_{pp}(\omega)\, e^{-\omega \frac{|r_x|}{\alpha_x U_c}} e^{-\omega \frac{|r_y|}{\alpha_y U_c}} e^{-j\omega \frac{r_x}{U_c}}, \quad (6)$$

plotted in Figure 3 (a) and a diffuse field [10]

$$S_{pp'}^{ac}(r_x, r_y, \omega) = A\, S_{pp}(\omega)\ \mathrm{sinc}\left(k_{ac}\sqrt{r_x^2 + r_y^2}\right), \quad (7)$$

showed in Figure 3 (b). The Corcos cross-spectrum (Eq. (6)) is composed of decreasing exponentials which describe the small spatial correlations of the pressures generated by the turbulences with the coefficients $\alpha_x = 8$ and $\alpha_y = 1$ [1, 11]. The diffuse field (Eq. (7)) represents the acoustic radiation of the turbulences. A is the energy ratio between the acoustic and aerodynamic components. This coefficient is set to 5% and corresponds to a particular case of TBL measured by Arguillat *et al.* [3]. Finally, the simplified model is given by

$$S_{pp'}(\omega) = S_{pp'}^{aero}(\omega) + S_{pp'}^{ac}(\omega), \quad (8)$$

and is plotted in Figure 3 (c).

The Cholesky decomposition is used in order to generate the excitation signals that comply with the cross spectrum of Eq. (8) for each frequency [12]. This method based on the decomposition of the cross-spectrum matrix given by Eq. (8) provides the random signals which are used to excite the plate in the direct problem.

3 Identification by inverse problem

The direct problem of a vibrating plate excited by the signals presented above is solved by modal decomposition. The plate corresponds to a vehicle windshield with $h = 3.85$ mm, $E = 70$ GPa, $\rho = 2700$ kg.m^{-3} and $\nu = 0.22$. Damping is artificially high to limit the computation time. For this case, the aerodynamic and acoustic coincidences are respectively $f_{conv} = 34$ Hz and $f_{ac} = 3.2$ kHz (Figure 2). To approach experimental conditions, a noise is added to vibration signals $w(x, y, \omega)$ with a Signal-to-Noise Ratio (SNR) equal to 50 dB.

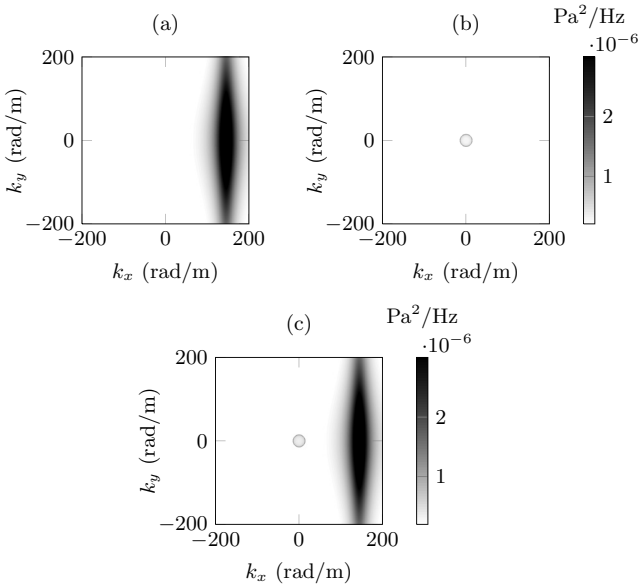

Figure 3: (a) Corcos, (b) diffuse field, (c) Corcos+diffuse field cross-spectra ($U_c = 35$ m.s^{-1}, $f = 800$ Hz).

Then the inverse problem can be applied. Initially, the FAT method is presented, then the results are shown before and around the acoustic coincidence ω_{ac} (Figure 2).

3.1 The Force Analysis Technique (FAT)

FAT is an inverse problem of vibration based on the equation of flexural motion Eq. (4) where the spatial derivatives of the measured displacement field are estimated by finite differences. They correspond to $\delta_{i,j}^{4x}$, $\delta_{i,j}^{4y}$ and $\delta_{i,j}^{2x2y}$ of Eq. (9) and are given in [4]:

$$p_{i,j}^{FAT} = D\left(\delta_{i,j}^{4x} + \delta_{i,j}^{4y} + 2\delta_{i,j}^{2x2y}\right) - \rho h \omega^2 w_{i,j}. \quad (9)$$

13 points of measured displacements around the point (i, j) are required to compute the spatial derivatives. As any inverse problem, FAT is very unstable and sensitive to the noise localized essentially in the high wavenumbers. To regularize, the identified pressure is windowed and filtered spatially with a cutoff filter

$$k_c^{FAT} = a \cdot k_f, \quad (10)$$

where a is generally equal to 1, 2, 3 or 4 depending on the noise level, 2 being a standard value.

In practice, the pressure is windowed by a Tukey function which weights the field over a width equal to $\lambda_c^{FAT} = \frac{2\pi}{k_c^{FAT}}$ at the edges of the reconstruction area. Then, a spatial convolution is applied between the identified pressure and a sinc function windowed by a Hanning function of length $2\lambda_c^{FAT}$.

3.2 Wall pressure identification before the acoustic coincidence

FAT is applied on the vibration signals of the plate excited by the Corcos and diffuse fields. Results are shown in Figure 4. The frequency spectra of the aerodynamic and the acoustic parts are plotted and they are obtained by the synthesis of signals presented above.

The curve called *inverse operator without noise* corresponds to the application of the inverse operator Eq. (9) on the noiseless displacement field and therefore without the

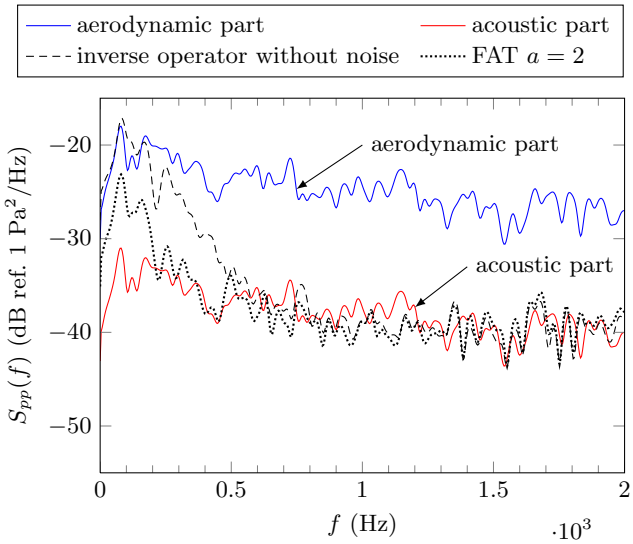

Figure 4: Frequency spectra of identified wall pressures where a noise is added to the displacement field (SNR = 50 dB).

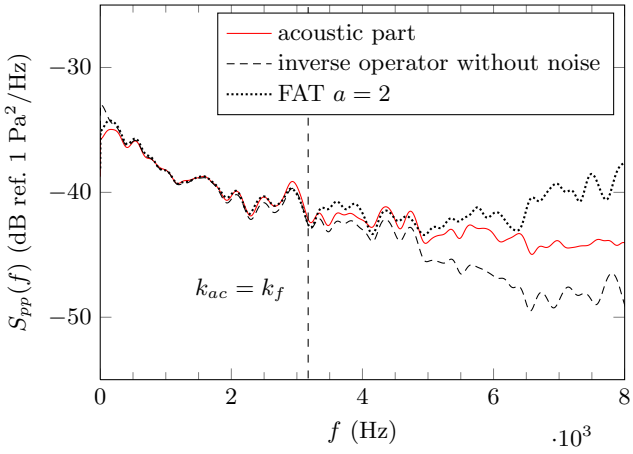

Figure 5: Frequency spectra of the identified wall pressures in higher frequencies (SNR = 50 dB).

regularization step. It is considered as the optimal solution of the FAT. It shows that FAT identifies only the aerodynamic part up to 200 Hz, and exclusively the acoustic part after 600 Hz. Between these two frequencies, the method identifies only a small part of the aerodynamic component.

If one can apply the perfect inverse operator of the motion equation Eq. (4), without spatial discretization, the inverse problem will identify fully the excitation, the aerodynamic and acoustic parts at all frequencies. But here, the spatial discretization in FAT associated with the inverse operator acts as a low-pass filter in the wavenumber domain. Leclère and Pézerat have showed in [13] that the cut-off number of this natural filter is around the flexural wavenumber. Thus, at low frequencies the method reconstructs well the aerodynamic and acoustic parts. With an aerodynamic coincidence being in the very low frequencies (f_{conv} = 34 Hz), when increasing the frequency, FAT is quickly unable to identify the aerodynamic part because it is filtered by the natural filtering of the method. In other words, the convective energy is too far from the circle of radius k_f in Figure 2. However, the acoustic component is located inside this circle up to the acoustic coincidence (f_{ac} = 3.2 kHz), and the method can reconstruct precisely the radiation part of the TBL.

The last curve of Figure 4 represents the pressures reconstructed by FAT from noisy signals. The same observations can be done, but unlike the previous case the regularizing filter with cut-off k_c^{FAT} can isolate earlier the acoustic from the aerodynamic at low frequencies.

3.3 Wall pressure identification around the acoustic coincidence

This section presents the application of FAT at higher frequencies. To reduce the computation time, the Corcos part is removed in the signal synthesis. Only the diffuse files Eq. (7) is kept since the aerodynamic part is not viewed by the method after 600 Hz. As before, Figure 5 shows the frequency spectra of the excitation, the optimal solution for FAT and the one identified for SNR = 50 dB.

The optimal solution is first analysed. The diffuse field can be reconstructed up to the acoustic coincidence, because the energy is contained within the circle of radius k_f. The natural filtering of the method cuts around the wavenumber k_f but the shape of this filter is set by the spatial discretization [13]. Here, the acoustic part can be identified up to 5 kHz.

For noisy signals, the inverse operator is applied using the FAT regularization. The latter allows one to reconstruct entirely the excitation up to about 5 kHz. In higher frequencies, the method takes into account too high wavenumbers according to Eq. (10). The influence of noise on the inverse problem is too important and the regularization is no longer effective. But anyway, at these frequencies, even the optimal solution can not properly reconstruct the acoustic energy.

4 Conclusion

In this study, a numerical experiment for the identification of wall pressures generated by TBL is performed. The synthesis of the excitation signals that comply with the model Corcos+diffuse field leads to solve the direct problem of vibration and then to test the inverse problem FAT. Results show that FAT identifies the acoustic component of the excitation that is usually very difficult to measure. Indeed, its level is much lower than that of the aerodynamic component. In addition, a microphone array of only 13 sensors is needed to apply this method without the need to modify the structure. The method is much easier to implement than other current techniques especially since the measurement can be made on the plate on the other side of the flow. In the near future, it is planned to make measurements of the displacement by a non-intrusive technique such as near-field acoustic Holography.

References

[1] W. K. Blake. *Mechanics of Flow-Induced Sound and Vibration, Vols. 1 and 2*. Academic Press, New York, 1986.

[2] M.S. Howe. Surface pressures and sound produced by turbulent flow over smooth and rough walls. *The Journal of the Acoustical Society of America*, 90:1041–1047, 1991.

[3] B. Arguillat, D. Ricot, C. Bailly, and G. Robert. Measured wavenumber: Frequency spectrum associated with acoustic and aerodynamic wall pressure fluctuations. *The Journal of the Acoustical Society of America*, 128:1647–1655, 2010.

[4] C. Pézerat and J.-L. Guyader. Force analysis technique: reconstruction of force distribution on plates. *Acta Acustica united with Acustica*, 86(2):322–332, 2000.

[5] Y. F. Hwang, W.K. Bonness, and S.A. Hambric. Comparison of semi-empirical models for turbulent boundary layer wall pressure spectra. *Journal of Sound and Vibration*, 319(1-2):199–217, 2009.

[6] W. R. Graham. A comparison of models for the wavenumber-frequency spectrum of turbulent boundary layer pressures. *Journal of sound and vibration*, 206(4):541–565, 1997.

[7] X. Gloerfelt. Spectre de pression pariétale sous une couche limite turbulente et rayonnement acoustique associé. CFA (Lyon, France), 2010.

[8] D. M. Chase. The character of the turbulent wall pressure spectrum at subconvective wavenumbers and a suggested comprehensive model. *Journal of Sound and Vibration*, 112(1):125–147, 1987.

[9] G. M. Corcos. Resolution of pressure in turbulence. *The Journal of the Acoustical Society of America*, 35:192–199, 1963.

[10] H. Nélisse and J. Nicolas. Characterization of a diffuse field in a reverberant room. *The Journal of the Acoustical Society of America*, 101:3517–3524, 1997.

[11] B. Arguillat. *Étude expérimentale et numérique de champs de pression pariétale dans l'espace des nombres d'onde, avec application aux vitrages automobiles*. PhD thesis, Ecole Centrale de Lyon, Laboratoire de Mécanique des Fluides et d'Acoustique, 2006.

[12] A. Hekmati, D. Ricot, and P. Druault. Vibroacoustic behavior of a plate excited by synthesized aeroacoustic pressure fields. AIAA/CEAS Aeroacoustics Conference, 2010.

[13] Q. Leclère and C. Pézerat. Vibration source identification using corrected finite difference schemes. *Journal of Sound and Vibration*, 331:1366–1377, 2012.